

This value can be obtained from the threshold pion photoproduction data and the Panofsky ratio. The current prediction²⁵ for this value is $(a_1 - a_3) = 0.245 \pm 0.010$. If we assume a linear momentum dependence for α_1 and α_3 , i.e., take only the first term in (12), the 31-Mev data yields a value $(a_1 - a_3) = 0.278 \pm 0.026$.

At 20.7 Mev the expression

$$\sigma_{\text{tot}} = (8\pi\lambda^2/9)(\alpha_1 - \alpha_3)^2 + 2(\alpha_{33} - \alpha_3)^2 + (\alpha_{31} - \alpha_{11})^2 \quad (13)$$

was solved for $(\alpha_1 - \alpha_3)$, assuming that the other phase shifts obeyed the momentum dependencies given above. The result was

$$(\alpha_1 - \alpha_3)/\eta = 0.272 \pm 0.025.$$

These values are in fair agreement with the prediction from the other low-energy data.

However, in order to make a proper comparison of these results, we must know the actual momentum dependence of the phase shifts from 0 to 30 Mev. Theoretically Cini *et al.*²⁶ have shown from crossing symmetry and Hamilton and Woolcock²⁵ from the finite momentum transfer dispersion relations of Chew, Low, Goldberger, and Nambu²⁷ that $(\alpha_1 - \alpha_3)$ is not linear in

²⁶ M. Cini, R. Gatto, E. L. Goldwasser, and M. A. Ruderman, *Nuovo cimento* **10**, 242 (1958).

²⁷ G. F. Chew, M. L. Goldberger, F. E. Low, and Y. Nambu, *Phys. Rev.* **106**, 1337 (1957).

η and that the value of $(a_1 - a_3)$ should be smaller than that obtained by a linear extrapolation.

In Fig. 9, a plot of α_1 and α_3 vs η is shown for a wide range of available data. The straight lines shown are those obtained from the combination *D* data of reference 5. A small nonlinear dependence may well be indicated by the data in Fig. 9. Thus, there is some indication on both theoretical and experimental grounds that the behavior of $(\alpha_1 - \alpha_3)$ is slightly nonlinear in the low-energy region. This would tend to improve the already reasonable agreement between $(a_1 - a_3)$ obtained from the linear extrapolation to zero energy of the scattering results reported in this paper, and the predictions from the other low-energy pion phenomena.

ACKNOWLEDGMENTS

The authors wish to express their gratitude to Professor S. W. Barnes for his advice and encouragement throughout this work. Many others at this laboratory have made contributions. In particular, we wish to thank Alex Wieber for his help in assembling and aligning the apparatus; Fred Palmer and the operating crew for the many hours of cyclotron operation; and the staff of the mechanical and electronics shops for their help in constructing and maintaining the equipment. One of us (K. Miyake) is indebted to the Fulbright Commission for a travel grant.

Investigation of Light Fragmentation Products and Peculiarities of Nuclear Fission at High Energies of Incident Particles

P. A. GORITCHEV, V. F. DAROVSKIKH, O. V. LOZHKIN, A. I. OBUKHOV, N. A. PERFILOV, AND U. P. JAKOVLEV
Radium Institute, Academy of Sciences, Leningrad, U.S.S.R.

(Received November 2, 1961)

Nuclear emulsions were used to study the charge spectrum of fragments and the multiplicity of fragment production in disintegrations of Ag and Br nuclei caused by incident 9-Bev protons. The paper contains some new results of investigation of fission of Pb, Bi, and U with 660-Mev protons.

I. INTRODUCTION

THE paper contains some new results of investigation of fission and fragmentation in nuclear emulsions. The advantages of observing individual disintegrations were used to study various correlations in fragmentation and fission processes to obtain additional data necessary to understand the mechanism of these processes.

The following features of fragmentation were investigated: 1. The dependence of the charge spectrum of fragments (with $3 \leq Z \leq 9$) on the amount of energy transferred to the nucleus by the incident proton, and on the direction of emission of fragments relative to

the incident proton direction. 2. Correlation of charges, energies, and angles of fragment emission in case of multiple fragment production.

The following features of fission of U, Bi, and Pb nuclei were studied: 1. The dependence of mean combined fragment range on the range ratio of light and heavy fission fragments. 2. The fission yields for Pb and Bi fission in relation to the range ratio. 3. The U and Bi fission anisotropy at the incident proton energy of 660 Mev.

The superfine grained *P-9(S)* emulsions were irradiated at Dubna with proton beams from the synchrotron (9 Bev) and synchrotron (660 Mev). The methods used are similar to those described in previous

TABLE I. Results of comparison of integral track width distributions in different disintegrations.

Characteristics of disintegrations with fragments			The number of investigated fragments		Mean value of integral track width ^a		Values of the probability p from comparison of two distributions ^c	
			Group I	Group II	Group I	Group II	Group I	Group II
Total number of charged particles in disintegration ^b	≤ 12	159	102	0.60	1.46	0.51	0.18	
	> 12	134	90	0.60	1.48			
Number of fragments with $Z \geq 4$ in disintegration	1	262	209	0.60	1.47	0.48	0.8	
	≥ 2	112	167	0.60	1.45			
The direction of fragment emission in relation to the primary	$N_f = 1$	$\leq 90^\circ$	150	130	0.59	1.49	...	0.6
		$> 90^\circ$	58	56	0.60	1.49		
	$N_f \geq 2$	$\leq 90^\circ$	112	95	0.63	1.49	...	0.4
		$> 90^\circ$	63	51	0.61	1.46		

^a The mean value of integral track width of fragments is given in arbitrary units for ranges $\geq 16\mu$ in the first group and $\geq 38\mu$ in the second group.

^b Only for disintegrations with one fragment.

^c p is the probability that because of statistical reasons the disagreement of the two distributions compared will be less than that observed.

papers.¹⁻³ The charge determination in the region $3 \leq Z \leq 9$ was made by measuring the track width with a special semiautomatic photometric device.

II. FRAGMENTATION

A. The Charge Spectrum of Fragments in Nuclear Disintegrations of Ag and Br Nuclei by 9-Bev Protons

Table I gives the results of two series of track width measurements of multicharged particles in different groups of Ag and Br nuclear disintegrations varying in the total number of emitted particles, in the number of particles with $Z \geq 4$, and in the direction of their emission in relation to the incident proton.

For each group of disintegrations the distributions of integral track widths of fragments were plotted. Two methods were used to check these distributions in the region $Z > 3$: the statistical method (the calculation of Pierson's χ^2 criterion) and the method of comparison of the mean track width distributions. Both methods of comparison (Table I) lead to the following results. The track width distributions and therefore the charge spectra of multicharged particles practically coincide for: (1) the disintegrations differing in energy transferred to the nucleus in the collision with the incident particle, (2) the disintegrations with different number of fragments, and (3) the disintegrations in which the fragments are emitted forward and those in which the fragments are emitted backward in relation to the incident beam.

Table II contains the charge spectra of fragments in different types of disintegrations. The integral charge

¹ N. A. Perfilov, N. S. Ivanova, O. V. Lozhkin., M. M. Makarov, V. I. Ostroumov, Z. I. Solovyova, and V. P. Shamov, J. Exptl. Theoret. Phys. (U.S.S.R.) **38**, 345 (1960).

² V. F. Darovskikh and N. A. Perfilov, J. Exptl. Theoret. Phys. (U.S.S.R.) **36**, 652 (1959).

³ A. I. Obukhov and N. A. Perfilov, J. Exptl. Theoret. Phys. (U.S.S.R.) **40**, 1250 (1961).

spectrum of fragments is shown in Fig. 1 (curve I). It should be noted that the results obtained here hold only for the charge region from 4 to approximately 8 and for that portion of the energy spectrum which includes the fragments with energies greater than 2 Mev per nucleon. No definite results can be stated for the low-energy portion of fragments and for fragments with big charges. However their relative yield is not large (about 7%) and, therefore, the results obtained can have more general application.

B. Some Features of Multiple Fragment Production

The distribution of disintegrations of Ag and Br nuclei observed in the emulsions with respect to the number of emitted fragments per disintegration is given in Table III.

As can be seen from Table III, multiple fragment production gives an appreciable contribution to the fragmentation process at 9-Bev incident proton energy. The measured relative probabilities of emission of various numbers of fragments per disintegration can be compared to the probabilities calculated on the assumption of their independent production.

TABLE II. The charge spectrum of fragments in different types of disintegrations (N_f , number of fragments; n , number of other charged particles).

Type of disintegration	Number of fragments					
	Be	B	C	N	$Z \geq 8$	
$N_f = 1$	$n \leq 12$	76	24	4	2	0
	$n > 12$	68	22	9	4	0
	Forward	102	34	11	4	0
	Backward	42	12	2	2	0
	Total	144	46	13	6	0
$N_f \geq 2$	Forward	67	29	14	1	1
	Backward	45	17	1	0	0
	Total	112	46	15	1	1

TABLE III. Distribution of disintegrations with respect to the number of fragments.

Type of disintegration \ N_f	1	2	3	4
Only with fragments with $4 \leq Z < 9$	~ 2000	289	35	2
Only with Li^8 fragments	153	4	1	0
One fragment is Li^8 , others with $4 \leq Z < 9$...	54	9	2
One fragment is B^8 , others with $4 \leq Z < 9$	14	4	3	2

In this case the ratios between numbers of disintegrations with various numbers of fragments are in first approximation given by the following relations:

$$N(2f)/N(1f) = N(3f)/N(2f) = N(4f)/N(3f) = p_2, \quad (1)$$

$$N(2\text{Li}^8)/N(1\text{Li}^8) = N(3\text{Li}^8)/N(2\text{Li}^8) = p_1, \quad (2)$$

$$N(1f + \text{Li}^8)/N(1f) = N(2f + \text{Li}^8)/N(2f) = N(3f + \text{Li}^8)/N(3f) = p_1, \quad (3)$$

$$N(2f + \text{Li}^8)/N(1f + \text{Li}^8) = N(3f + \text{Li}^8)/N(2f + \text{Li}^8) = p_2, \quad (4)$$

where p_1 is the probability of Li^8 emission in a disintegration, and p_2 is the probability of emission of fragments with $Z \geq 4$ in a disintegration. p_1 and p_2 were calculated as a ratio of corresponding cross sections to the total cross section of inelastic interaction of 9-Bev protons with Ag and Br nuclei.

For row (1), we have obtained the experimental values 0.14, 0.12, 0.06 which coincide with $p_2 = 0.09$ within statistical errors. This value also does not disagree with the values of row (4): 0.17, 0.22, because of poor statistics.

For row (2), we have the values of ratios 0.026 and 0.25, and for row (3), 0.030, 0.032, 0.057, which somewhat exceed the value $p_1 \approx 0.01$, but are in good agreement with each other [except the ratio $N(3\text{Li}^8)/N(2\text{Li}^8)$, which is, however, statistically unreliable].

Thus the study of relative probabilities of observation of various numbers of fragments per disintegration evidently does not disagree with the assumption that they are independently emitted in disintegrations with several fragments.

(1) Disintegrations with Two Fragments

As has been already mentioned, the charge spectrum in the case of multiple fragment emission is essentially the same as in the case of single fragment emission. This point leads directly to the conclusion that the relative probabilities for the emission of particular fragments are independent of the emission of other fragments in the same processes.

The charge spectra for disintegrations with one fragment and for those with two fragments will co-

incide if the probability of observation of the pair of charges Z_n and Z_m in one disintegration is equal to the product of probabilities of emission of each charge:

$$p_{nm} = p_n p_m.$$

Then if $\sum_n p_n = 1$ and $\sum_m p_m = 1$, the probability of observation of fragments of charge Z_n in disintegrations with two fragments can be found as

$$P_n = \sum_m p_m p_n = p_n \sum_m p_m = p_n;$$

i.e., it occurs with a probability equal to the probability of observation of charge Z_n in disintegrations with one fragment.

Figure 1 presents the relative frequencies of observation of the couple of charges Z_n and Z_m in one disintegration with respect to their sum ($Z_n + Z_m$) and the frequency of observation of two fragments of the same charge with respect to the charge of the fragment. These data were derived from the study of 36 disintegrations in which the charges of both fragments could be measured. The same figure gives the calculated probabilities p_{nm} for these two cases, obtained on the assumption of independent production of fragments. It can be seen that the experimental values p_{nm} and p_{nn} are in accordance with calculated values.

The distribution of spatial angles between two fragments shown in Fig. 2 was obtained from the measurement of angles in 303 disintegrations. The distinct angular correlation of fragments in these disintegrations can be seen: Fragments are preferentially emitted with angles $> 120^\circ$ between them. No dependence of the mean angle between the fragments on the sum of

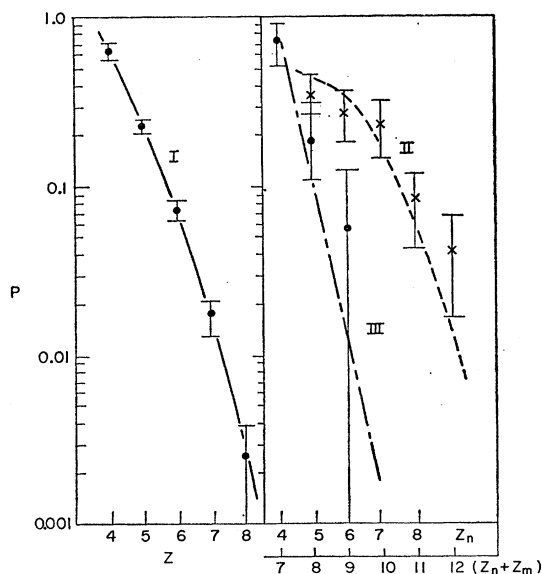


FIG. 1. Curve I—the charge spectrum of fragments in disintegrations of Ag and Br nuclei. Curve II—the probability of emission of fragments with charges Z_n and Z_m as a function of the sum ($Z_n + Z_m$). \times , experiment; dashed line, calculation. Curve III—the probability of emission of two fragments with equal charges Z_n plotted against Z_n . \bullet , experiment; dash-dotted line, calculation.

their charges was found. With values of 6 to 10 for the sum of the charges, the mean angle between the fragments remains about 110° .

In Fig. 2 the dashed line shows the distribution of spatial angles between two fragments in case of independent production. This distribution was calculated using the Monte Carlo method. The angular distribution was taken from Perfilov *et al.*¹ Contrary to the experimentally observed angular distribution this calculated distribution has a minimum in the region 150° – 180° and fills the interval 0 – 30° in which no events were found.

The energy distributions of fragments in disintegrations with $N_f=2$ for charges 4, 5, and 6 are given in Fig. 3. The same figure shows the distribution of the ratio of energy per nucleon for the heavy to that for the light fragment emitted in one disintegration. The energy distributions of such fragments appear to be similar to those observed in disintegrations with one fragment,¹ and the most probable ratio of energies per nucleon in heavy and light fragments is about unity. Both these facts also agree with the assumption of independent emission of fragments in such disintegrations.

2. Disintegrations with Three Fragments

The poor statistics of disintegrations with three fragments (44 events) did not permit any detailed investigation of the characteristics of such disintegrations. The most reliable data could be obtained for angular distributions of fragments in these disintegrations. Figure 4 shows the distribution of projections of angles between adjoining fragments in disintegrations with three fragments. The prevalence of large angles between the fragments can clearly be seen. For disintegrations with three fragments the expected distribution

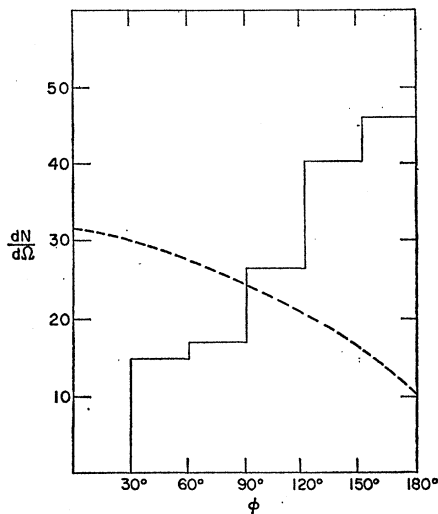


FIG. 2. The distribution of spatial angles (ϕ) between two fragments. Histogram, experimental results; curve, calculation for independent fragment emission.

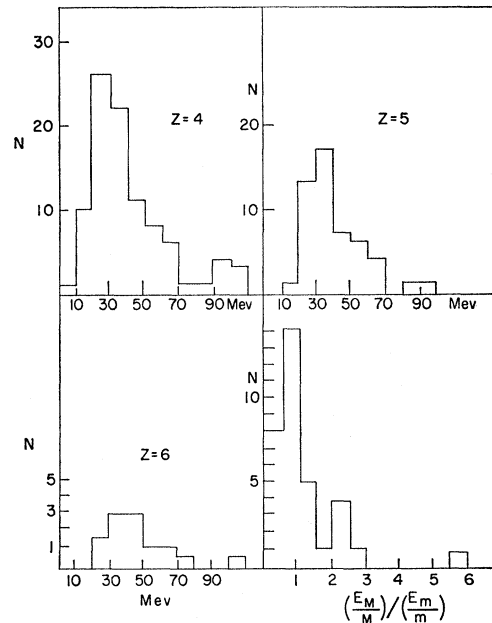


FIG. 3. Energy distributions of fragments in disintegrations with two fragments for $Z=4, 5,$ and 6 and the ratio of energy per nucleon in heavy to that in light fragments $[(E_M/M)/(E_m/m)]$.

of angle projections between adjoining fragments can be calculated under the assumption of independent production according to the formula given by Lovera⁴ (the dashed line in Fig. 4). Clearly, the experimentally obtained distribution differs essentially from this calculated one.

The measurement of fragment charges in these disintegrations gave the following result for $Z \geq 4$ fragments: the numbers of fragments with charges 4, 5, 6, and 7 are, respectively, 18, 9, 2, and 1. Within the statistical errors these relative numbers are compatible with the integral charge spectrum for disintegrations with $N_f=1$ and $N_f=2$ (Fig. 1).

C. Some Remarks on the Mechanism of the Fragmentation Process

Some conclusions about the mechanism of the process leading to the emission of fragments can be drawn from the analysis of the data obtained here.

The fact that the charge spectrum of fragments does not depend on the value of energy transferred to the nucleus, nor on the number of fragments, nor on the direction of their emission makes the often used assumption of several mechanisms (such as knock-on process, evaporation, and fission) being responsible for the emission of fragments, each contributing to the cross section for fragmentation, improbable. Because the charge spectrum preserves its form in a broad

⁴ G. Lovera, Nuovo cimento 6, 233 (1949).

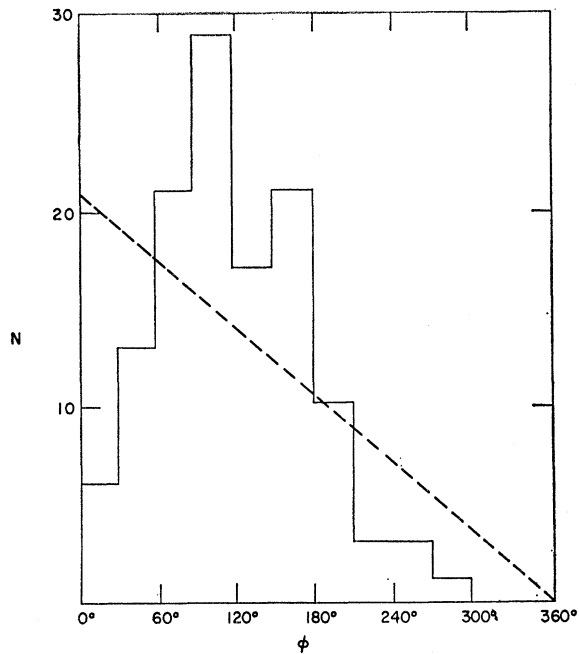


FIG. 4. The distribution of projections of angles (ϕ) between the fragments in disintegrations with 3 fragments. Histogram, experimental data; dashed line, calculation for independent fragment emission.

region of energies of incident particles,^{5,6} one may surmise that the emission of fragments takes place as a result of one mechanism of nuclear disintegration, independent of the energy of the incident particle. The investigation of some features of multiple production of fragments leads one to suggest a possible mode of the process of fragment emission. As has already been mentioned, the relative probabilities of the emission of various numbers of fragments and the correlation of their charges and energies are in good accord with the hypothesis of independent emission of particular fragments. At the same time, angular correlations of fragments in disintegrations with two and three fragments are in visible disagreement with this hypothesis. The situation will not change even if the Coulomb interaction between fragments is introduced.

However, we cannot reject the hypothesis of independent fragment emission merely on the basis of the fact that the fragments are correlated in angles; rather we have to try to understand this fact in the framework of the independent-fragment-emission model. The problem of angular correlation requires a certain model, but other characteristics of independent fragment emission do not.

There are two possibilities of explanation. In the model of fragment production during the development

⁵ O. V. Lozhkin, N. A. Perfilov, A. A. Rimski-Korsakov, and J. Fremlin, *J. Exptl. Theoret. Phys. (U. S.S.R.)* **38**, 1958, 1388 (1960).

⁶ N. A. Perfilov, O. V. Lozhkin, and V. P. Shamov, *Uspekhi Fiz. Nauk.* **70**, 3 (1960).

of the cascade process in the nucleus (both on the assumption of quasi-elastic collisions of cascade nucleons with clusters^{1,5} and on the assumption of bond-breaking in the nucleus during the cascade process),⁷ the existence of angular correlation of emitted fragments requires an assumption of spatial nonuniformity in the distribution of clusters of nucleons within the nucleus; the probability of two large clusters of nucleons in close proximity to each other in the nucleus is small. Thus, the emission of fragments will take place from widely separated regions of the nucleus and this will lead to large angles between emitted fragments. The other possibility of explanation of angular correlation of fragments will appear if we assume that the fragments can be formed as a result of the so-called rapid breakup of a nucleus, characteristics of which are determined by the statistical distribution of energy and momentum between the products of disintegration before they leave the volume where the interaction between them took place. In this case the angular correlations of fragments are due to the laws of conservation.

It is difficult to make a final choice between these two models at present. Further accumulation of experimental data and development of methods of calculation of these processes are necessary.

III. FISSION

A. The Range Characteristics of Fission of Lead Nuclei by 660-Mev Protons

In order to investigate the dependence of the combined kinetic energy of fission fragments on the asymmetry of fission, the mean combined range of fission fragments was plotted against the range ratio of light

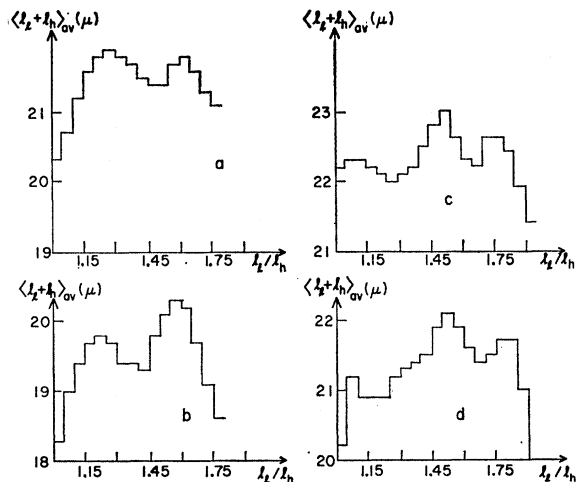


FIG. 5. The mean combined range of fission fragments as a function of the range ratio. Lead: a—1- and 2-prong events; b— ≥ 3 -prong events. Bismuth: c—1-, 2- and 3-prong events; d— ≥ 4 -prong events.

⁷ P. P. Denisov, K. V. Kosareva, and P. A. Čerenkov, *Proceedings of Conference on the Peaceful Uses of Atomic Energy*, Tashkent, 1961.

and heavy fragments. The relationships obtained are given in Fig. 5. Curve (a) corresponds to the emission of one and two charged particles, and curve (b) corresponds to the emission of three and more charged particles, (p or α) in fission events. The curves were statistically treated by the Ferreyra-Valoshek method.⁸ Both figures show similar patterns in the range ratio region from $l_l/l_h=1$ to $l_l/l_h=2$; the mean combined range has two maxima at $l_l/l_h \approx 1.25$ and $l_l/l_h \approx 1.6$. So at these values of range ratio the mean combined kinetic energy of fission fragments reaches two maxima. Figure 5 also presents similar curves for Bi obtained in an earlier work.²

To evaluate the effect of the velocity of the recoiling nucleus on the observed phenomena the dependence of the mean combined range on the range ratio was plotted for two groups of events. All the fission events were divided into two groups: The first one included those events where the fission fragment with the longer range was emitted forward (in relation to the incident direction); the second group included those events in which such a fragment was emitted backward. In the first group the velocity of the recoiling nucleus increased the range ratio; in the second group it decreased the range ratio.

Figure 6 shows the corresponding curve (statistically treated by the Ferreyra-Valoshek method). It can be seen that the positions of the maximum values of the mean combined kinetic energy are the same for the first and the second group. Therefore, it can be concluded that the velocity of the recoiling nucleus has a negligible effect upon these characteristics.

In Fig. 7, histograms of the distribution of fission events with respect to the range ratios are presented. It can be seen that in the events in which a small number of charged particles are emitted, fission is symmetric.

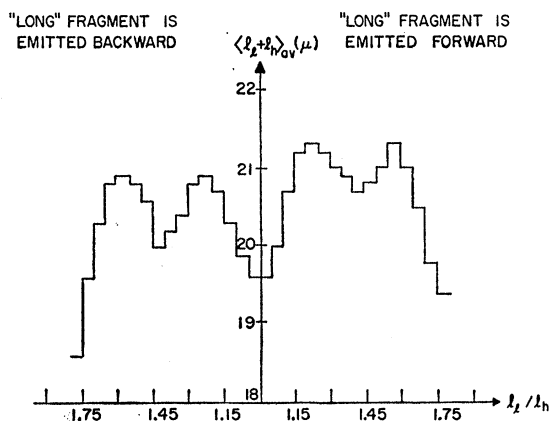


FIG. 6. The mean combined range of fission fragments as a function of the range ratio for different directions of "long"-fragment emission.

⁸ Ferreyra, Valoshek, *Proceedings of the International Conference on the Peaceful Uses of Atomic Energy*, Geneva, 1955 (United Nations, New York, 1956), Vol. 2, p. 1076.

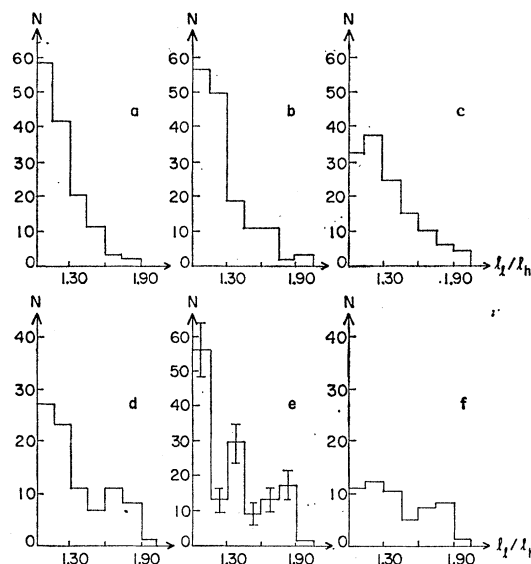


FIG. 7. The frequency of lead fissions as a function of the range asymmetry. The different histograms correspond to fission events with different prong numbers: a—0; b—1; c—2; d—3; e—4, 5; f— ≥ 6 prong events.

In events where 4 or 5 charged particles are emitted [Fig. 7(e)] a distinct maximum of asymmetric fission at $l_l/l_h \approx 1.37$ can be observed together with the symmetric fission pattern. There is perhaps a third maximum at $l_l/l_h \approx 1.82$. The χ^2 test shows that the probability of such a pattern occurring due to statistical fluctuations is less than 0.02. It is clear that the statistical errors are not responsible for the observed form of the curve, and there exists asymmetric fission for this group of fission events with appreciable probability.

As for the fission events accompanied by six or more charged particles, nothing definite can be stated because of poor statistics.

Figure 8 presents similar histograms for Bi, which shows the same fission pattern.

By analysis of the data for Bi and Pb it is possible to give a reasonable explanation for the observed effects, assuming that a large enough fraction of fission events takes place after the excitation energy is almost completely dissipated, i.e., from the lowest level from which fission can occur.

Fission events occurring at higher excitation levels will, of course, blur the existing effects.

In cases when fission occurs in a "cold" nucleus there must be a parallel in the mechanism of kinetic energy release between uranium fission initiated by particles of low energies and lead and bismuth fission by high-energy particles. In the case of uranium fission by low-energy particles the increased kinetic energy release is observed when one of the fission fragments is a nucleus with filled shell⁹ ($N=82$, $N=50$, $Z=50$).

⁹ A. N. Protopopov, I. A. Baranov, Y. A. Selitzki, and V. P. Eismont, *J. Exptl. Theoret. Phys. (U.S.S.R.)* **36**, 1932 (1959).

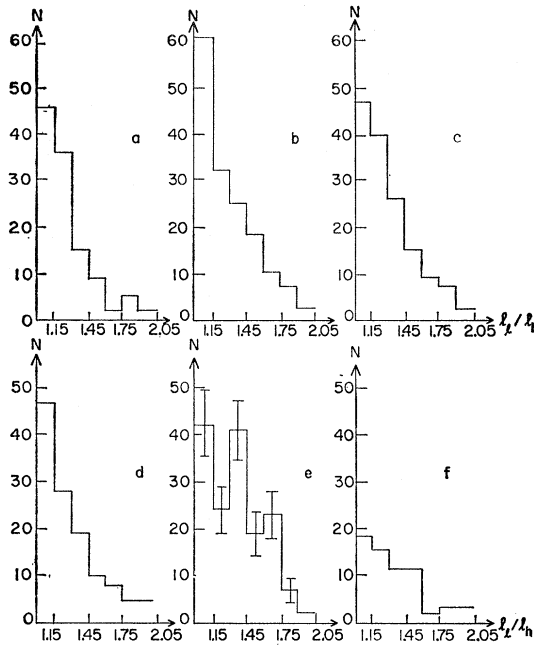


FIG. 8. The frequency of bismuth fissions as a function of the range asymmetry. a—0; b—1; c—2; d—3; e—4, 5; f— ≥ 6 prong events.

A similar consideration can be applied in our case. Let us find out in which region of mass ratios one would expect maxima in the values of combined kinetic energy for Pb and Bi. If a fragment has 50 neutrons then it will correspond to almost symmetric fission, because the complementary fragment will contain less than 75 neutrons (some of the neutrons are evaporated during the process of excitation energy release).

The range ratio of light- and heavy-fission fragments must be in the region of $1 < l_l/l_h < 1.30$. The presence of 82 neutrons in one fragment corresponds to a number of neutrons in the other fragment which is less than 43, i.e., the range ratio $l_l/l_h \geq 1.65$. Finally a maximum of combined kinetic energy release should be observed

when one of the fragments has 50 protons. This corresponds to $Z < 32$ for the complementary fragment, and the range ratio $1.3 < l_l/l_h < 1.65$.

Approximately, such a pattern exists in reality for Pb and Bi (Fig. 5). The maximum value of $\langle l_l + l_h \rangle_{av}$ corresponding to $N_Z = 50$ is observed for Pb at $l_l/l_h \approx 1.6$ and for Bi at $l_l/l_h \approx 1.52$. In case of Bi there was observed one more peak in the value of $\langle l_l + l_h \rangle_{av}$ at $l_l/l_h \approx 1.77$ (corresponding to $N_N = 82$). In case of Pb a similar peak coincides with the neighboring peak, which is due to the $N_Z = 50$ shell. The observed maxima of $\langle l_l + l_h \rangle_{av}$ in the region of $l_l/l_h \approx 1.25$ must correspond to $N_N = 50$. In case of Bi we have observed a certain increase of combined mean range for fission near the symmetric region.

The appearance of an asymmetric fission peak on the curve of yields of Pb fission accompanied by emission of 4 and 5 charged particles looks very interesting [Fig. 7(e)]. A similar effect was observed² earlier for Bi [Fig. 8(e)]. The appearance of this peak was explained in connection with the presence of 50 and 28 proton shells in fission fragments. This explanation might be true for Pb also.

B. Anisotropy of Angular Distribution of the Products of Fission of U and Bi by 660-Mev Protons

The results of the investigation of the angular distribution of fission fragments relative to the direction of the primary are given in Table IV. The values given for the anisotropy in spatial distribution of fission fragments were calculated from the experimentally observed distribution of projected directions of fission fragment trajectories on the emulsion surface.³

The results for U do not support the large anisotropy in the angular distribution of fragments [$W(90^\circ)/W(0^\circ) = 1.33 \pm 0.19$], previously obtained by us.¹⁰

To obtain data on angular momentum received by a nucleus during interaction with an energetic proton, the calculation of momenta was made using the results

TABLE IV. Angular distribution of fission products.

	U+n, 14 Mev Total	Bi+p, 660 Mev Total	Total	U+p, 660 Mev $n_{ap}=0$	$n_{ap} \geq 1$
Number of fission events	3130	5650	4441	2083	2358
Excitation energy (Mev)	18.8	170 ± 25	140 ± 15	85 ± 20	170 ± 25
Type of angular distribution	$W(\theta) = 1 + B \cos^4 \theta$		$W(\theta) = 1 + C \sin^2 \theta$		
Anisotropy	$B = 0.46 \pm 0.11$	$C = 0.02 \pm 0.06$	$C = 0.04 \pm 0.07$	$C = 0.05 \pm 0.11$	$C = 0.01 \pm 0.10$

TABLE V. Forward-to-backward asymmetry of "light" fragments in the lab system.

Range asymmetry	1.00-1.10	1.10-1.20	1.20-1.40	1.40-3.20	1.00-3.20
(Forward/backward) _{exp}	1.20 ± 0.07	1.44 ± 0.09	1.45 ± 0.19	2.10 ± 0.14	1.52 ± 0.03
(Forward/backward) _{calc}	1.25	1.50	1.83	2.17	1.69

¹⁰ O. V. Lozhkin, N. A. Perfilov, and V. P. Shamov, J. Exptl. Theoret. Phys. (U.S.S.R.) **29**, 292 (1955).

of the cascade process calculation for U.¹¹ The angular momentum of the nucleus in this calculation was assumed to be equal to the difference between the orbital momentum brought in by the incident particle and the combined momentum of emitted cascade particles:

$$\mathbf{M}_n = \mathbf{M}_0 - \mathbf{M}_k = [\mathbf{r}_0 \cdot \mathbf{P}_0] - \sum_k [\mathbf{r}_k \cdot \mathbf{P}_k],$$

where \mathbf{P}_0 and \mathbf{P}_k = momenta of incident proton and emitted charged particle; \mathbf{r}_0 = vector of the first interaction of incident proton with a nucleon in a nucleus; \mathbf{r}_k = vector of the last interaction before emission of cascade particle.

According to this calculation, the mean angular momentum of the nucleus after the cascade amounts to about one third of the mean value of orbital momentum brought in by the incident proton ($34\hbar$). There is a wide range of orientation of nuclear momenta in contrast to the perpendicular orientation with respect to the incident beam in the case of compound nucleus formation (Fig. 9).

According to Bohr¹² and Halpern and Strutinsky,¹³ the anisotropy in the angular distribution of fission fragments occurs in the case when there is an advantageous orientation of angular momenta of nuclei and when the excitation energy at the moment of fission is low enough. The disorientation of angular momenta of nuclei, due to the cascade process and perhaps the high excitation energy at the moment of fission, make the angular distribution of fission fragments nearly isotropic (Table IV).

One other possible type of anisotropy in the angular distribution of fission fragments was studied, i.e., a deficiency of light (or heavy) fragment emission forward or backward in the center-of-mass system. This type of anisotropy can be characterized by the forward-to-backward ratio (in the center-of-mass system), of longer-range (light) or shorter-range (heavy) fragments.

¹¹ N. S. Ivanova and I. I. Pyanov, J. Exptl. Theoret. Phys. (U.S.S.R.) 31, 416 (1956).

¹² A. Bohr, *Proceedings of the International Conference on the Peaceful Uses of Atomic Energy, Geneva, 1955* (United Nations, New York, 1956), paper No. 911.

¹³ I. Halpern and V. M. Strutinsky, *Proceedings of the Second United Nations International Conference on the Peaceful Uses of Atomic Energy, Geneva, 1958* (United Nations, Geneva, 1958), paper No. 1513.

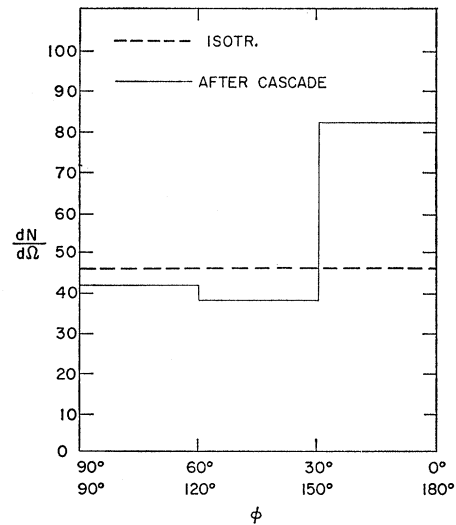


FIG. 9. Orientation of angular momenta of U nuclei after the cascade process ($E_p=660$ Mev).

In the lab system the addition of the recoil velocity of the nucleus before fission leads to an increase (in relation to the center-of-mass system) of the number of fragments (light as well as heavy) in the forward direction. This effect of the recoil velocity is relatively greater for the longer-range fragments.

In Table V the ratios of the number of longer-range fragments emitted forward to the number of those emitted backward are given for several intervals of asymmetry of the ranges of fragments of U fission by 660-Mev protons. The values of these ratios calculated on the assumption of equal probability of fragment emission forward and backward are also presented. As can be seen, the experimental values coincide with calculated ones within the statistical errors.

ACKNOWLEDGMENT

The authors are greatly indebted to Professor G. Friedlander of Brookhaven National Laboratory for his invaluable help during the preparation of the manuscript for publication and his English corrections in the text.